Photonic Localization and Positioning using Multi-Tone Continuous-Wave Ranging Methodology

Mustafa Mert Bayer
University of California, Irvine
5109 Engineering Hall
UCI, Irvine, CA 92697
bayerm@uci.edu

Ataberk Atalar
University of California, Irvine
5109 Engineering Hall
UCI, Irvine, CA 92697
aatalar@uci.edu

Xun Li
University of California, Irvine
5109 Engineering Hall
UCI, Irvine, CA 92697
xunl12@uci.edu

Haoyu Xie
University of California, Irvine
5109 Engineering Hall
UCI, Irvine, CA 92697
xieh10@uci.edu

Ozdal Boyraz
University of California, Irvine
4420 Engineering Hall
UCI, Irvine, CA 92697
oboyraz@uci.edu

Abstract— We propose and demonstrate autonomous photonics localization and navigation system that does not require any time clocks at the transmitter and the receiver. Experimentally we show that a remote receiver that is 2km away from the transmitter determines its relative location to the transmitter with a better 3cm standard deviation and successfully identifies 10cm incremental changes in distance without using time information. The proposed concept is based on Multi-Tone Continuous Wave ranging technology that uses a transmitter consisting of an amplitude-modulated CW laser by the phase-locked multiple RF tones. The receiver side consists of a heterodyne detection system with a free-running local oscillator laser and signal processing algorithms that eliminate phase noise and relative decoherence of two independently free-running lasers and identifies relative phase changes between RF tones and potential Doppler shifts The proposed technology is proven to be suitable for long-range localizations, autonomous navigations of aerial or ground-based vehicles such as rovers or drones for space missions, as well as helping to maintain inter-satellite navigation, and even aiding during the landing of a spacecraft. The proposed architecture has the ability to operate in the near and far-field by optimizing the optical power dynamics and RF tone selections and overcoming the laser phase-noise limitations.

TABLE OF CONTENTS

1. INTRODUCTION

The importance of accurate location and velocity tracking has been an important subject since World War II for militaries due to the usefulness it provides for targeting, navigation, and planning. The first satellite-based tracking method which is called the global positioning system (GPS) was developed towards the end of the 20th century under the name of navigation satellite timing and ranging system (NAVSTAR) by the US Department of Defense [1]. Over the years, the advancements in GPS technology have created a wide range of civilian and military applications in numerous fields, such as transportation [2], geophysical exploration, agriculture, and even structural health monitoring. Recently, there is a growing interest in chip-scale photonics positioning, navigation, and timing (PNT) [3] for interior and exterior implementations such as visible-light-based applications for indoor navigation and photonics-based multiple-input-multiple-output radar for navigation purposes [4], [5]. Moreover, previous applications utilized CCD cameras [6], [7], frequency combs via microresonators [8], and ultra-narrow linewidth lasers [9] to realize photonics-based localization. Often, these techniques rely on synchronized clocks or synchronized multiple transmitters.

As an alternative to the conventional PNT techniques, we present a clock-free high-precision approach for photonics localization and positioning, where a single free-running optical transmitter (Tx) is employed without the need for any type of time synchronization with the receiver (Rx). In this technique, we utilize the relative variations on the phases of sidebands of an amplitude-modulated CW optical carrier. In particular, we amplitude modulate a CW laser by multiple phase-locked radio-frequency (RF) tones by using an electro-optic modulator (EOM) at the transmitter side. While the multi-tone modulated CW (MTCW) light propagates from the transmitter to the receiver, each modulation frequency accumulates a different phase based on the propagation distance. The received modulated beam is optically convolved with an independent free-running local oscillator on the Rx side for heterodyne detection to enhance the signal-to-noise ratio (SNR) of the system. As long as the frequency differences between the two lasers lie within the detector bandwidth, it is possible to distinguish the frequency-shifted sidebands. Then, digital bandpass filters near the RF tones can be used to get the waveforms of the

2023 IEEE Aerospace Conference | 978-1-6654-9032-0/23/$31.00 ©2023 IEEE | DOI: 10.1109/AERO55745.2023.10115739

978-1-6654-9032-0/23/$31.00 ©2023 IEEE

individual tones. However, each filtered waveform will have a common phase-noise contribution from both the Tx and Rx laser sources. To eliminate these, we perform common-noise elimination by RF mixing the filtered individual RF tones to generate the noise-free intermediate frequencies (IF). Then, the target distance can be computed through a series of post-processing and triangulation algorithms by exploiting the redundancy generated by multiple IFs [10].

The working principle of the MTCW PNT is derived from the previously demonstrated Phase-Based MTCW lidar technique [11]–[14], where the plurality of sidebands carried by the laser is used to acquire the target distance by utilizing their phases and frequencies. The ability of common-noise elimination through RF mixing of the stable RF tones enables ranging beyond the coherence length of the employed laser in the MTCW lidar configuration. A similar approach is used in the MTCW PNT architecture to facilitate high SNR measurements via an optical local oscillator, where the phase noises of the two lasers are eliminated through RF mixing of the static sidebands.

To prove the concept, a testbed is constructed with a Tx that has the modulated CW signal and a receiver side with an independent laser. A pseudo 1.8km distance is created by using a ~1.2km fiber spool in between Tx and Rx. Along with high-frequency tones that yield higher positioning resolution, low-frequency tones are utilized to achieve coarse positioning, as well. Experimentally we demonstrate that the photonic MTCW positioning method can locate targets with ~10cm separation and <3cm precision at a 1.8km distance. It is further possible to transmit additional information such as timing, coordinates, etc. by encoding the relevant information to the modulation frequencies.

The proposed signal processing technique, which can be used in either the digital or analog domain, eliminates the common phase noise of lasers and thus provides the proposed MTCW PNT with the capability of ultra-long-range localization, despite the laser coherence length. This opens the door for the realization of navigation, localization, and positioning that are not affected by the imperfections and restrictions of reference clocks. The potential applications of the system are broad, from improving the accuracy of GPS systems to enabling autonomous navigation of aerial or ground-based vehicles such as rovers or drones for space missions, as well as helping to maintain inter-satellite navigation, and even aiding during the landing of a spacecraft with respect to a reference transmitter. The proposed architecture has the ability to provide service for both near and far-field applications by optimizing the optical power dynamics and RF tone selections and overcoming the laser phase-noise limitations.

2. THEORETICAL MODEL

The proposed architecture for photonics PNT via the MTCW approach is presented in Figure 1. The CW laser operating at a frequency of ω_t on the transmitter side is modulated by a Mach-Zehnder modulator (MZM) that operates at the quadrature bias. A total of N number of synthesized phase-locked RF frequencies (f_i) is fed to the input port of the MZM after an RF combiner. The modulation generates sidebands in the optical spectrum as $\omega_t \pm \omega_i$, where $\omega_i = 2\pi f_i$. To acquire the coarse range information, considering the 2π-cyclic behavior of the phase, a low modulation frequency in the kHz range is also utilized by RF mixing with one or multiple of the high-frequency modulations. The low-frequency components have a longer unambiguous range to determine the coarse position of the target, while the high-frequency tones perform localization with higher accuracy.

The modulated signal is pulsated via an EOM to realize higher peak powers. Then the MTCW signal is amplified and transferred to the free space via a collimator (CL). The electric field equation of the propagating beam based on the total propagation distance is given in Eq.(1). Here, A_t is the amplitude of the transmitted light, m is the modulation index, α_t is the linear attenuation, ϕ_i^{RF}, ϕ_0^t, and $\phi_n^t(t)$ are the initial RF phase, initial carrier phase, and the laser phase noise, respectively. The transmitted light is collected by the CL of the Rx side after propagating a distance L with the speed of light, c.

$$E_t = A_t\alpha_t \exp\left[j\omega_t t + j\phi_0^t + j\omega_t \frac{L}{c} + j\phi_n^t(t) \right] - \frac{m}{2} A_t\alpha_t \sum_{i=1}^{N} \left(\begin{array}{l} \exp\left[\begin{array}{l} j(\omega_t+\omega_i)t + j\phi_0^t + j\phi_i^{RF} \\ +j(\omega_t+\omega_i)\frac{L}{c} + j\phi_n^t(t) \end{array} \right] \\ +\exp\left[\begin{array}{l} j(\omega_t-\omega_i)t + j\phi_0^t - j\phi_i^{RF} \\ +j(\omega_t-\omega_i)\frac{L}{c} - j\phi_n^t(t) \end{array} \right] \end{array} \right) \quad (1)$$

Then the beam is convolved with a local oscillator that has a frequency of ω_r to strengthen the collected modulation tones through a heterodyne detection system. The electric field of the laser in the receiver can be formalized as in Eq.(2) , where A_r, ϕ_0^r and $\phi_n^r(t)$ are the amplitude, initial phase, and the laser phase noise, respectively.

$$E_r = A_r \exp(j\omega_r t + j\phi_0^r + j\phi_n^r(t)) \quad (2)$$

The local oscillator is a free-running laser without any frequency and phase locking to the remote transmitter. Hence, time synchronization is not necessary to perform the positioning of the Rx. The resultant beam is transmitted to the photodetector (PD) to generate the photocurrent (I_{pd}) as given in Eq.(3),

$$I_{pd} = I_{DC} + 2\alpha_m A_t A_r \cos\left((\omega_t - \omega_r)t + \omega_t \frac{L}{c} + \Phi + \phi_n^t(t) - \phi_n^r(t) \right) - \frac{m}{2}\alpha_m A_t A_r \left[\begin{array}{l} \sum_{i=1}^{N} \cos\left(\begin{array}{l} (\omega_t - \omega_r + \omega_i)t + (\omega_0 + \omega_i)\frac{L}{c} \\ +\Phi + \phi_i^{RF} + \phi_n^t(t) - \phi_n^r(t) \end{array} \right) \\ +\sum_{i=1}^{N} \cos\left(\begin{array}{l} (\omega_t - \omega_r - \omega_i)t - (\omega_0 - \omega_i)\frac{L}{c} \\ +\Phi - \phi_i^{RF} - \phi_n^t(t) - \phi_n^r(t) \end{array} \right) \end{array} \right] \quad (3)$$

where I_{DC} is the DC portion of the photocurrent and the self-beating terms are neglected for simplicity. Also, the initial

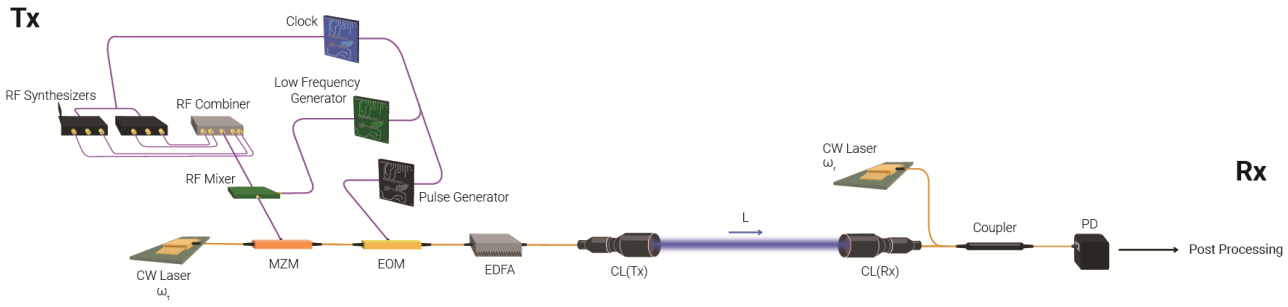

Figure 1. Schematic of the proposed phase-based multi-tone continuous-wave GPS positioning architecture with transmitter and receiver sides.

phase difference of the optical carriers is defined as $\Phi = \phi_0^t - \phi_0^r$.

It is possible to locate the shifted tones with apriori knowledge of the preselected tone frequencies, after data acquisition. In the resultant spectrum, the highest peak power will be realized at ω_t-ω_r and it is possible to use this peak as a reference to locate the modulation tones. Then, digital bandpass filters near the RF tones can be employed to generate the filtered waveforms of the individual tones. However, each resultant peak will have a contribution of phase noise from Tx and Rx lasers. To eliminate these, tones $\omega_t - \omega_r \pm \omega_i$ are RF mixed with the $\omega_t - \omega_r$. Then the phase-noise-free tones are RF mixed with each other to generate noise-free intermediate frequency (IF) components have the formalism of $A_i A_j \cos\left(\Delta\omega_{i,j} t \pm \Delta\phi_{i,j}\right)$, where $\Delta\phi_{i,j}$, and $\Delta\omega_{i,j}$ are the phase and frequency differences of i^{th} and j^{th} tones ($i \neq j$), respectively. Furthermore, the target distance can be computed by using Eq.(4), where n is an integer.

$$L = \frac{\left(2\pi n + \Delta\phi_{i,j}\right)c}{\Delta\omega_{i,j}} \tag{4}$$

By using the results generated by multiple tones, it is possible to triangulate the L by sweeping the potential n values and seeking a common solution that satisfies the phase results of all $\Delta\omega_{i,j}$. The triangulation algorithm sorts the potential distance results in a matrix. For each $\Delta\omega_{i,j}$, the results are stored inside the corresponding column of a data matrix, and the standard deviation (σ) of each row of the calculated potential distances is computed by the algorithm. As a result, the mean value of the row with the lowest standard deviation indicates the measured ΔL. In other words, the solutions of Eq.(4) for each $\Delta\omega_{i,j}$ for different n values should converge to the same ΔL, which corresponds to the output with the lowest standard deviation. The details of the triangulation process along with the utilized algorithms for the MTCW lidar application are presented in [11], [12].

Moreover, the repetitive nature of the phase will generate the unambiguous range as $L_u = 2\pi c / \omega_{gcd}$, where ω_{gcd} is the greatest common divisor of $\Delta\omega_{i,j}$. The mixing of the synthesized RF tones with a low-frequency modulation paves the way to enhance the range of the system by lowering the ω_{gcd} to kHz levels. In such a configuration, where one of the tones is RF mixed with a kHz level f_{low}, the unambiguous range will be determined by the f_{low}, and the new L_u will be defined as $L_u = c/2f_{low}$. Here, up and down-shifted mixed frequencies ($f_i \pm f_{low}$) are evaluated separately by filtering and RF mixing $f_i + f_{low}$ with f_i - f_{low} to acquire the coarse range information using Eq.(4). Then, the fine ranging is performed using all the $\omega_t - \omega_r + \omega_i$ or $\omega_t - \omega_r - \omega_i$ depending on the availability of the bandwidth.

3. Numerical Verification

To demonstrate the concept and provide an understanding of the triangulation, we performed a numerical verification by using Eq.(1) and Eq.(2) to mimic the behavior of light in the software domain. In the simulations, the time window is set to be 1024μs with 2^{22} samples per run which yield a 244ps time resolution. In addition, the corresponding bandwidth is

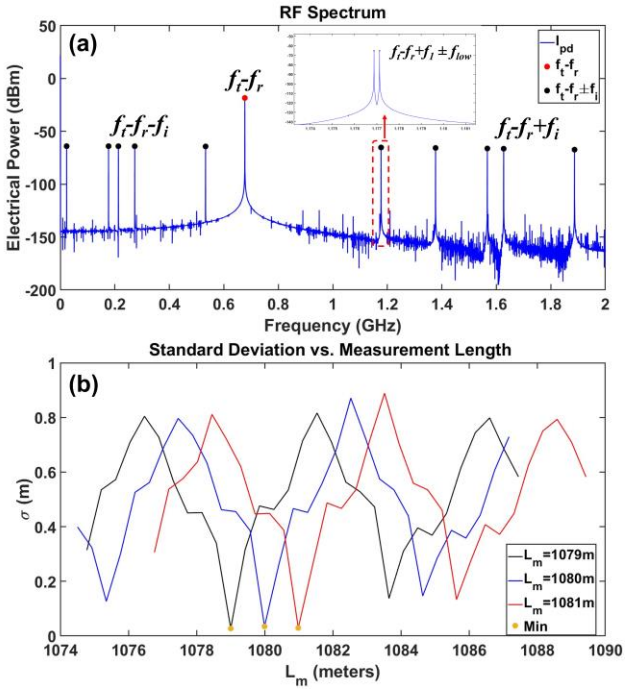

Figure 2. Simulation results. (a) The resultant photocurrent spectrum with the subcarrier modulation is indicated in the inset. (b) The result of the triangulation algorithm for three consecutive distances.

2GHz with a frequency resolution of ~1kHz. The arbitrary frequency difference between lasers of Tx and Rx is randomly selected to be 677MHz with the consideration of the bandwidth requirements. In addition, the central wavelength is set to 1064nm. The Tx side is modulated via an MZM with a modulation index of $m = 0.01$. The selected phase-locked RF frequencies are 500, 700, 890, 950, and 1210MHz, which are selected in a fashion to forestall potential second harmonic or cross-beating overlaps. For the purpose of coarse ranging, a low frequency at 125kHz is employed and it is opted to be RF mixed with the 500MHz tone to realize the subcarrier modulation. The output power of the system is set to 30dBm and a 40dB loss is introduced to the optical path between Tx and Rx. On the receiver side, the Rx laser is set to operate with a 0 dBm optical output power. The received Tx signal is coupled with the unmodulated Rx signal on the photodetector to generate the photocurrent, I_{pd}. The detector noises such as the shot noise, thermal noise, and dark current, as well as the nonlinear effects, are neglected for simplicity and proof of concept purposes.

The unambiguous range with the employed 125kHz subcarrier modulation corresponds to 1.2km indicating the maximum range for localization with the MTCW approach. Therefore, the Rx is arbitrarily set to be stationed at three locations with a 1m separation, which are 1079m, 1080m, and 1081m, respectively. The selected positions are within the unambiguous range based on the selected parameters.

The simulation results are presented in Figure 2. The resultant I_{pd} spectrum is shown in Figure 2(a). Here, the peak with the maximum power exhibits due to the frequency difference between the two laser sources corresponding to 677MHz. The upshifted and downshifted frequencies are indicated, as well. The subcarrier modulation applied to the 500MHz tone (f_1) is further indicated in the inset, where the frequency difference between f_t-f_r+f_1+f_{low} and f_t-f_r+f_1-f_{low} is 250kHz. These two terms are RF mixed and the phase and the frequency of the noise-free resultant IF signal are used in Eq.(4) to compute the coarse range. After getting an understanding of the coarse position of Rx, the possible integer values of n for each IF term are calculated for a ±10m range around the coarse position. Then, the triangulation algorithm is applied using Eq.(4) using the determined n values. The triangulation algorithm sorts the potential distance results in a matrix to compute the standard deviation of each row to find the common solution of ΔL for each $\Delta\omega_{i,j}$. The results of the triangulation operation for three consecutive Rx positions are displayed in Figure 2(b). The minimum standard deviation points are indicated with yellow circles. The measured distances are 1079.0m, 1079.9m, and 1080.9m, respectively. Moreover, the ideal minimum standard deviation in Figure 2(b) is if all the solutions of Eq.(4) converge exactly to the same ΔL. Therefore, the value of the minimum σ_{min} yields the accuracy of the measurement, which depends on the systematic errors of the system such as clock drifts, timing jitter, etc.

The resolution of the acquired position information is defined by the phase resolution of the system, which is defined by the time resolution of the measurement. In the simulation, time resolution, dt, is 244ps. The positioning resolution can be formalized as $\delta L = c \times dt$ which corresponds to 7.3cm for the simulation which is the minimum theoretical resolution achieved by the MTCW PNT approach. The factors such as measurement accuracy depend on the factors such as sampling rate, jitter, total noises in the system, etc. Furthermore, positioning precision is described by the SNR of the architecture which is related to the detection electronics.

4. Experimental Setup

The experimental setup in Figure 3 is built to test the capability of the MTCW localization methodology. Two separate laser sources are used in the Tx and Rx. The utilized lasers are manufactured by RPMC Lasers Inc. (R1064SB0300PA) and they are set to operate at around ~1064nm with <100kHz laser linewidth. The spectral difference between the two lasers is set to be <1GHz by fine-tuning the operating temperature of both sides to satisfy the bandwidth requirements. The Tx side power is set to be 10.2mW, while Rx operates at ~2.5mW. In the transmitter, the laser is followed by an MZM (iXblue -NIR-MX-LN-10-PD-P-P-FA-FA) that has a 10GHz modulation bandwidth and 30dB extinction ratio. The MZM is biased at the quadrature point with 5.8V. We used 4 phase-locked RF modulation frequencies at 500, 700, 890, and 950MHz produced by RF synthesizers (Windfreak Technologies - Synth Hd) that have the same 10MHz reference clock. For coarse target ranging, a low-frequency generator is employed

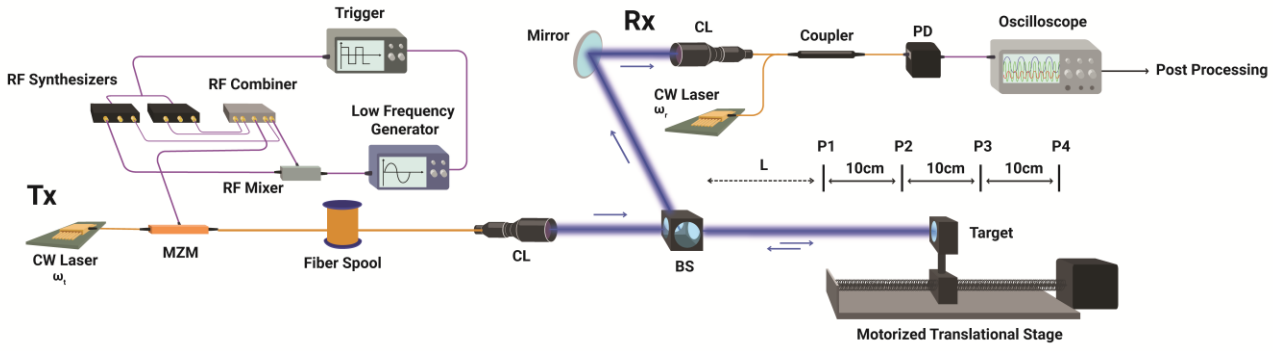

Figure 3. Experimental setup to test the MTCW localization system.

to supply a 500kHz frequency to be RF mixed with the 500MHz tone. The low-frequency tone is also phase-locked with the high-frequency tones by using a subharmonic of the 10MHz reference clock.

We introduced a ~1.2km long fiber spool to mimic the long-distance propagation of light in the free space. Intending to control the range of the target, we utilized a motorized translational stage to establish four different target positions that are separated by 10cm distances. The target reflector is moved on the stage after 10 measurements are performed on each location. For collection purposes, a polarization-insensitive beamsplitter (BS) is placed in between the Tx collimator (CL) and the target reflector to transmit the echo signal from the target to the Rx collection lens. The collected light is fiber-coupled, which is further interfered with the Rx local oscillator laser. The resultant optical signal is fed to the PIN photodetector (PD) with ~2.5GHz bandwidth to generate the I_{pd}. For data acquisition, a digital storage oscilloscope (Tektronix – TDS7704B) is employed that has a 7GHz bandwidth with a 20GSa/s sampling rate. The time window of the measurement is set to 100μs and the time resolution is 100ps. Similarly, the corresponding measurement bandwidth is 5GHz with a 10kHz frequency resolution. 10 trials are performed at each location and the triangulation algorithm is applied to the acquired data.

The post-processing starts with the interpolation of the data to improve the time resolution of the system to 23.8ps. Furthermore, we perform the isolation of the f_t - f_r peak, which has the strongest peak in the spectrum. After filtering the laser peak using a Butterworth bandpass filter that preserves the phase information, the measured data is digitally RF mixed with the filtered data. The resultant IF term possesses noise-free sidebands that shifted back to their original values. Then each modulation tone is individually filtered and RF mixed. The phase and frequency information of the IF values of the RF mixed sidebands are stored for the triangulation algorithm. The low-frequency components at 500MHz ± 500kHz are utilized to estimate the coarse range information, while the RF tones are used to pinpoint the position of the target. Using the potential n values acquired from the coarse ranging, triangulation is performed. Moreover, the Tx is calibrated prior to the measurements to acquire the initial tone phases to prohibit potential distortions due to residual RF phases caused by the synthesizers.

5. Results and Discussion

After data acquisition, a Fast Fourier Transform (FFT) is performed on the interpolated time domain I_{pd} signal to acquire the spectrum of the raw data. The raw data spectrum of one of the measurements, while the target is at P_1, is presented in Figure 4(a). Here, the f_t - f_r peak is indicated with the red dot on the spectrum and it corresponds to 589MHz. Hence, the modulation sidebands are shifted as much as f_t - f_r. Using this peak and the apriori-knowledge of the static tone frequencies, the tones are localized on the RF spectrum and marked as black dots on the spectrum. The 700MHz tone is portrayed in the inset of Figure 4(a). This tone is shifted to ~1289MHz and accumulates the phase noise generated by both Tx and Rx lasers.

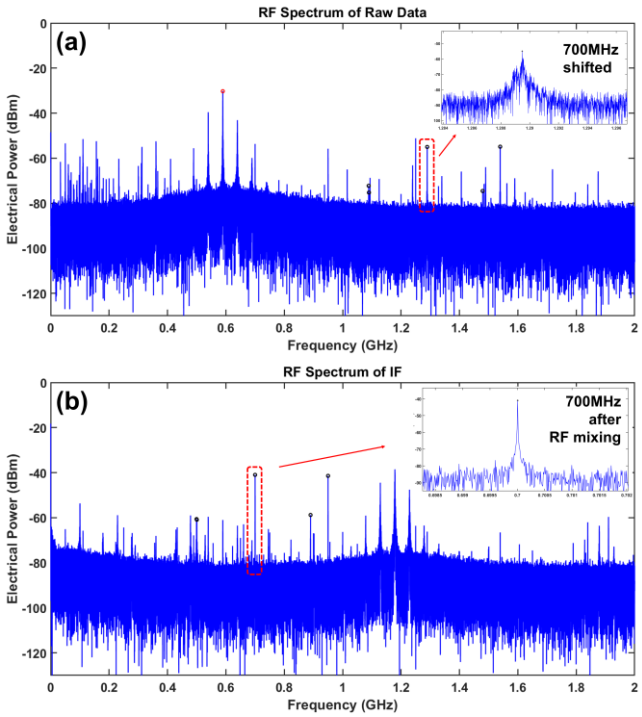

Figure 4. Simulation results. (a) The resultant photocurrent spectrum with the subcarrier modulation indicated in the inset. (b) The result of the triangulation algorithm for three consecutive distances.

To eliminate the common noise terms on the sidebands, the measured I_{pd} signal is RF mixed with the filtered $f_t - f_r$ peak (red dot). A 20MHz Butterworth bandpass filter center at 589MHz is utilized to isolate the $f_t - f_r$ peak. The resultant spectrum of the RF mixed signal is depicted in Figure 4(b). In the IF spectrum, the imperative sidebands shift back to the baseband, hence the corresponding peaks are stationed at their original preset frequencies. The 700MHz tone after RF mixing is presented in the inset of Figure 4(b). When both insets of Figure 4 are compared, it is evident that the phase noise induced by the Tx and Rx lasers diminishes after RF mixing of the I_{pd} with filtered $f_t - f_r$ signal. This can also be seen in Eq.(3). Same phase noise components are present in both the carriers and sidebands. Therefore, the resultant IF signal shifts back to the baseband with the common phase noise terms of the modulation frequencies being eliminated. On the other hand, the measurements are performed for 4 positions P_1, P_2, P_3, and P_4, respectively. Each position has a ~10cm separation and 10 measurements are performed at each location. The 10cm displacement corresponds to a ~20cm light propagation when the roundtrip from the target to the BS is considered. The introduced fiber spool is ~1.2km and by considering the refractive index of the fiber, the actual path becomes ~1800m in free space. Moreover, there is the free-space propagation of light, as well as the additional fibers in the system such as couplers, collimator fiber, MZM fiber, etc. that introduce additional propagation distance to the light. To estimate the actual path that is traveled by the light, we used a pulse to perform a pulsed time-of-flight (ToF) measurement. As a result, it takes ~6.08μs for the Tx

laser to reach the PD, which corresponds to ~1825±0.40m of total propagation distance.

To compute the coarse ranging, we utilized the ±500kHz subcarrier modulation on the 500MHz RF tone. The unambiguous range corresponds to ~300m based on $L_u = c/2f_{low}$. Since $L_m > L_u$ we assume apriori knowledge of the whereabouts of the target, meaning that the signal will complete 5 cycles ($n = 5$) for the low-frequency components. The coarse-ranging yields an estimated range of 10-40m and by assuming $n = 5$, the coarse position is found to be between 1810-1840m by utilizing the subcarrier modulation. In actual practice, it is possible to improve the L_u by employing multiple low-frequency components and adjusting the time window of the acquisition accordingly or by having apriori knowledge of the coarse position of the target.

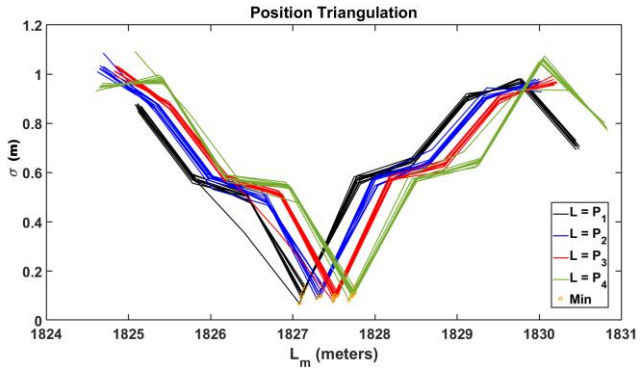

Figure 5 – Results of position triangulation for the target stationed at 4 different locations separated by ~10cm difference. Each color represents a position.

The high-resolution ranging is performed by utilizing the high-frequency sidebands (black dots in Figure 4(b)). The complete position triangulation results are presented in Figure 5 as previously discussed in Figure 2(b). Here, black, blue, red, and green colors correspond to P_1, P_2, P_3, and P_4 respectively. The minimum standard deviation points indicate the measurement distance in that trial, which is illustrated by yellow circles in Figure 5. The average measured distances are 1827.18m, 1827.34m, 1827.52m, and 1827.73m, respectively. In addition, the displacement between each position is measured as 21.9cm, 18.3cm, and 20.8cm, respectively. The errors in the displacement can be attributed to potential thermal variations in the long fiber and human error during the placement of the target.

The standard deviation of each set of 10 trials is measured as 2.3cm, 2.7cm, 2.0cm, and 2.1cm, respectively for the corresponding positions, which indicates the precision of the MTCW localization technique at >1.8km. The precision of the system depends on the SNR of the system. The SNR depends on the utilized bandwidth, and since only the phase and frequency information of the modulation sidebands are required, it is possible to utilize narrow bandpass filters around the tones to enhance the SNR of the system [12]. Nonetheless, further analysis is required to determine the limits of the MTCW localization system.

Moreover, the range resolution, δL, of the system depends on the phase resolution of the system, which also depends on the time resolution as $\delta L \sim \frac{d\phi_i}{\omega_i} c = dt \times c$. Here, the dt is enhanced by data interpolation to 23.8ps which yields a <1cm ranging resolution.

Furthermore, the accuracy of ranging depends on systematic errors such as clock errors, jitter, errors induced by the measurement electronics, etc. The accuracy of the MTCW localization can be estimated by checking the value of the minimum standard deviation (σ_{min}) point. In an ideal errorless scenario, the expected σ_{min} is 0m. Therefore, the deviations measured in σ_{min} can give an estimate of the accuracy of the measurement. In the experiment, the σ_{min} is measured as <10cm. The accuracy can be improved by improving the measurement electronics by reducing systematic errors.

7. Conclusion

In this work, we demonstrate photonics positioning and localization based on MTCW ranging system. The Tx and Rx have separate free-running lasers to enhance the SNR by employing optical heterodyne detection. Phase and frequency information of multiple static RF tones are utilized on the optical carrier to perform ranging of the target. In order to verify the theoretical work simulation results are presented. Moreover, we experimentally demonstrate a working example of the MTCW localization architecture that can localize closely spaced stationary targets over a long distance (~2km) with a precision of <3cm. The same technique has been utilized to measure dynamic targets in a lidar system [12]. The proposed technique can be used for future applications in localization and navigation technologies that require fine position information over long distances such as navigation of rovers or drones in space missions, inter-satellite navigation, and guidance during the landing of a spacecraft

Acknowledgments

We acknowledge the Office of Naval Research (N00014-18-1-2845) for their partial support in this research.

References

[1] G. Mintsis *et al.*, "Applications of GPS technology in the land transportation system," *Eur. J. Oper. Res.*, vol. 152, pp. 399–409, 2004.

[2] A. Amini *et al.*, "Improving GPS-based vehicle positioning for Intelligent Transportation Systems," in *Proc. IEEE - Int. Veh. Sym. 2014*, Ypsilanti, MI, USA, 2014, pp. 1023–1029.

[3] R. Lutwak, "Micro-technology for positioning, navigation, and timing towards PNT everywhere and always," in *Proc. ISISS* 2014, Laguna Beach, CA, USA, 2014, pp. 1–4.

[4] Z. Li *et al.*, "Fusion of Visible Light Indoor Positioning and Inertial Navigation Based on Particle Filter," *IEEE Photonics J.*, vol. 9, no. 5, pp. 1–13, Oct. 2017.

[5] F. Zhang *et al.*, "Photonics-based MIMO radar with high-resolution and fast detection capability," *Opt. Express,* vol. 26, no. 13, pp. 17529–17540, Jun. 2018.

[6] R. Mautz and S. Tilch, "Survey of optical indoor positioning systems," in Proc. *2011 Int. C. Indoor. Posit.*, Guimaraes, Portugal, Sep. 2011, pp. 1-7.
[7] W. M. Owen, "Methods Of Optical Navigation," Jet Propulsion Lab., Pasadena, CA, USA, Tech. Rep. AAS 11-215, 2011.
[8] Y. L. Li, "Photonic Systems Engineering: A Structured Approach to Positioning, Navigation and Timing using Microresonators," in *Proc. CLEO 2021*, San Jose, CA, USA, 2021, p. JTu1I.1.
[9] D. J. Blumenthal, "Integrated Ultra-Narrow Linewidth Ultra-Stable Brillouin Lasers and their Application to PNT Applications," in *Proc. CLEO 2021*, San Jose, CA, USA, 2021, p. JTu1I.3.
[10] M. M. Bayer *et al.*, "Photonics PNT Based on Multi-Tone Continuous Wave Ranging," in *Proc. CLEO 2022*, San Jose, CA, USA, 2022, p. JTh3A.57.
[11] M. M. Bayer and O. Boyraz, "Ranging and velocimetry measurements by phase-based MTCW lidar," *Opt. Express*, vol. 29, no. 9, pp. 13552–13562, Apr. 2021.
[12] M. M. Bayer *et al.*, "Single-shot ranging and velocimetry with a CW lidar far beyond the coherence length of the CW laser," *Opt. Express*, vol. 29, no. 26, pp. 42343–42354, Dec. 2021.
[13] M. M. Bayer *et al.*, "Simultaneous ranging and velocimetry with multi-tone continuous wave lidar," *Opt. Express*, vol. 28, no. 12, Jun. 2020.
[14] M. M. Bayer *et al.*, "Enhancing the multi-tone continuous-wave lidar with phase detection," in *Proc. SPIE-ODS 2021*, San Diego, CA, USA, 2021, vol. 11828, p. 1182807.

BIOGRAPHY

Dr. Mustafa Mert Bayer *received his B.S. degree in electrical engineering, and M.S. degree in optoelectronics and photonics engineering from Koc University, Turkey. He received his Ph.D. degree from UC Irvine. He is currently working as a postdoctoral fellow at UC Irvine. His work includes lidars, photonic Doppler velocimetry, and free-space optical communication. He developed amplitude-based and phase-based multi-tone continuous-wave (MTCW) lidar technology, which enables ranging beyond the coherence length of the lasers for CW lidars. The same technology establishes the basis for the MTCW positioning, navigation, and timing technique.*

Ataberk Atalar *received his B.S. and M.Sc. degrees in physics from Middle East Technical University (METU), Turkey. He is currently pursuing his Ph.D. degree at UC Irvine. His research interests include terahertz spectroscopy, fiberoptic vibration, acoustic sensors, free-space optical communication, ultrafast laser systems, lidars, and photonics-based positioning, navigation, and timing systems based on a novel approach named multi-tone continuous wave (MTCW) technology which makes it possible to obtain measurements beyond the CW laser coherence length.*

Xun Li *received his B.S. degree in material science and engineering from the Southern University of Science and Technology, China. Currently, he is a Ph.D. student in electrical engineering at UC Irvine. His work includes free-space optical communications, ray tracing & self-alignment simulations, and lidars. During his Ph.D., he developed a prototype of an ultra-long-range (>6km) free-space data communicator with multi-level self-alignment algorithms.*

Haoyu Xie *received his B.S. degree in electrical engineering from Chongqing University, China. He is currently studying as an M.S. student in the electrical engineering department at UC Irvine. His research interests include lidar, beam-steering systems, and free-space optical communication.*

Prof. Ozdal Boyraz *received his M.S. and Ph.D. degrees from the University of Michigan, Ann Arbor, in 1997 and 2001, respectively. After two years of industrial work at Xtera Communications, Allen, TX, he joined the University of California, Los Angeles as a postdoctoral fellow in 2003. After leading pioneering work on silicon photonics and optical signal processing techniques based on time-stretched systems at UCLA, he joined the University of California, Irvine as an assistant professor at the EECS department in 2005. He continues to work as a full professor at UC Irvine at present. His research areas include silicon-based optoelectronic devices, microwave photonics, optical communication systems, optical signal processing, free-space optical communications, and lidars. He is a recipient of the 2004 UCLA Chancellor Award and the DARPA Young Faculty Award in 2010.*